Reliability of the Mouse Model of Choroidal Neovascularization Induced by Laser Photocoagulation

Stephen H. Poor, Yubin Qiu, Elizabeth S. Fassbender, Siyuan Shen, Amber Woolfenden, Andrea Delpero, Yong Kim, Natasha Buchanan, Thomas C. Gebuhr, Shawn M. Hanks, Erik L. Meredith, Bruce D. Jaffee, and Thaddeus P. Dryja

Novartis Institutes for Biomedical Research, Cambridge, Massachusetts, United States

Correspondence: Stephen H. Poor, Novartis Institutes for Biomedical Research, 500 Technology Square, Cambridge, MA 02139, USA; Stephen.poor@novartis.com.

Submitted: June 20, 2014
Accepted: August 25, 2014

Citation: Poor SH, Qiu Y, Fassbender ES, et al. Reliability of the mouse model of choroidal neovascularization induced by laser photocoagulation. *Invest Ophthalmol Vis Sci*. 2014;55:6525–6534. DOI:10.1167/iovs.14-15067

Purpose. We attempted to reproduce published studies that evaluated whether the following factors influence choroidal neovascularization (CNV) induced by laser photocoagulation in murine retinas: small interfering RNA (siRNA), cobra venom factor, complement factors C3 and C5, and complement receptor C5aR. In addition, we explored whether laser-induced CNV in mice was influenced by the vendor of origin of the animals.

Methods. Reagents or genotypes reported by others to influence CNV in this model were assessed using our standard procedures. Retrospective analyses of control or placebo mice in many experiments were done to evaluate whether the CNV area induced by laser photocoagulation varied according to vendor.

Results. Administration of the following agents did not have a substantial impact on the CNV induced by laser burns in mice: siRNA, low-molecular-weight inhibitor of the C5a receptor (PMX53), or cobra venom factor. Jackson Laboratory (JAX) mice lacking either C3 or C5 had increased neovascularization compared to non-littermate JAX wild-type controls. Taconic mice lacking C3 had reduced CNV compared to non-littermate Taconic wild-type control mice. A retrospective analysis of vehicle-treated wild-type C57BL/6 mice used as controls across 132 experiments conducted from 2007 to 2010 revealed that mice purchased from JAX or from Charles River produced less neovascularization than mice from Taconic.

Conclusions. We present our recommended methods for conducting experiments with the mouse laser-induced CNV model to enhance reproducibility and minimize investigator bias.

Keywords: choroidal neovascularization, laser, mice, VEGF

Since its first description in 1987,[1] there have been numerous published experiments dealing with the choroidal neovascularization (CNV) that arises within a week or two after a laser pulse ruptures Bruch's membrane. Laser-induced CNV models have been developed for mice, rats, and monkeys. These animal models are highly relevant for CNV that occasionally occurs in human eyes after accidental laser burns.[2] Laser-induced CNV models provided preclinical evidence to support the clinical evaluation of anti-VEGF drugs for ocular neovascular diseases such as neovascular age-related macular degeneration (AMD) and diabetic retinopathy.[3] Because of their success in predicting the efficacy of anti-VEGF drugs, laser-induced CNV models have been used by numerous academic groups and pharmaceutical companies to learn about the underlying pathological mechanisms of neovascular AMD and to evaluate new therapies for ocular neovascular diseases.

In this report, we describe experiments designed to test some agents or genotypes that are reported to influence the area of CNV in the mouse laser-induced CNV model. The published studies that we selected for replication were chosen because the rationale for the experiments appeared to be logical based on associated results in the same papers or based on background knowledge of the relevant pathways.[4–7] The published findings apparently provided major insights into the possible origins of AMD, and these reports were accordingly published in journals with high-impact factors. Because of the importance of these results in understanding the cause of AMD, we attempted to replicate the published experiments as closely as possible to validate the findings. We additionally studied sources of variability in the mouse laser-induced CNV model, such as whether the vendor source of the mice influenced the results and whether there was variation associated with the idiosyncratic differences in the administration of the laser burns by different scientists. We provide our recommendations for improving the reproducibility of the model.

Methods

Type, Origin, and Selection of Mice

All study mice were female unless specifically indicated to be male. We used C57BL/6 mice that were typically 8 to 10 weeks old (range, 7–14 weeks). C57BL/6NTac mice were purchased from Taconic (Tarrytown, NY, USA), C57BL/6NCrl mice from Charles River Laboratories (Wilmington, MA, USA), and C57BL/6J mice from The Jackson Laboratory (JAX, Bar Harbor, ME, USA). In the data presented, the mice were purchased from Taconic unless otherwise stated. Mice used in a single experiment arrived at our research facility in a single shipment and were age-matched. Experimental interventions for a cohort of animals were started on the same day. Laser application for an individual

experiment was performed by a single scientist. Cages were randomly assigned to treatment groups with mice sharing a cage and receiving the same treatment. Animal research presented in this paper was approved by the Novartis Institutes for Biomedical Research IACUC Committee and adhered to the Association for Research in Vision and Ophthalmology Statement for the Use of Animals in Ophthalmic and Vision Research.

Laser Photocoagulation

Mouse pupils were dilated with 1 drop (volume, ~40 μL) of 1% cyclopentolate. Just before anesthesia was administered, pupil dilation was maximized with an additional drop of phenylephrine (usually 10% but occasionally 2.5% depending upon availability). Mice were then anesthetized with an intraperitoneal (IP) injection of a mixture of ketamine and xylazine at doses of 80 to 100 mg/kg and 5 to 10 mg/kg, respectively, or with 3-tribromoethanol at a dose of 200 to 250 mg/kg. Prior to laser pulse application, each eye was anesthetized with topical 0.5% proparacaine. Lubricating eyedrops (Genteal; Alcon Laboratories, Fort Worth, TX, USA) on a glass cover slip were applied to the cornea, and the retina was viewed through a slit lamp microscope. Each laser pulse was applied approximately 0.5 to 1 mm from the optic nerve; single pulses in each of 3 separate locations were applied to each eye for a total of 6 laser photocoagulation sites for each mouse. The pulses were from a green laser (wavelength, 532 nm; Oculight GLx model, Mountain View, CA, USA) and had a duration of 30 ms, a power of 120 mW, and a spot size of 100 μm. One laser instrument was used for all laser CNV studies presented in this report. A successful laser pulse generated a yellow vaporization bubble which correlated with a rupture of Bruch's membrane (evaluated histologically in control mice sacrificed 6 hours after lasering; data not shown). In cases when a vaporization bubble did not form (<1% of laser pulses), one additional laser pulse could be administered to the same spot. For each eye, a maximum of 4 laser pulses were allowed to generate 3 lesions. After the application of laser burns to both eyes, antibiotic ointment (tobramycin or neomycin ophthalmic ointment, depending on availability and cost) was applied to both eyes.

Tissue Processing, Imaging, and CNV Area Quantification

Unless otherwise indicated, analysis of neovascularization was completed for tissues harvested 7 days after laser photocoagulation. On the final study day, 0.1 mL of a 5 mg/mL solution of FITC concanavalin-A (Vector Laboratories, Burlingame, CA, USA) was injected intravenously (IV) to fluorescently label vascular endothelium. Animals were euthanized 15 to 30 minutes later by using inhaled carbon dioxide. Eyes were enucleated and fixed in 4% paraformaldehyde (Vector Laboratories) for approximately 60 minutes at room temperature, and then the fixative was replaced with phosphate-buffered saline (PBS). Each eye was assigned a randomized number to mask the samples for the remainder of the analysis. Posterior segments were isolated, and retinas were removed. The posterior eye cups, which included the retinal pigment epithelium (RPE), the choroid, and the sclera, were flat-mounted onto microscope slides after making 3 or 4 radial cuts. Fluorescence photographs of each CNV lesion were made with an Axiocam MR3 camera on an Axio Image M1 microscope (Carl Zeiss Microscopy, Thornwood, NY, USA). CNV area was quantified using a semiautomated analysis program (Axiovision software version 4.5, Carl Zeiss Microscopy) that outlined the fluorescent blood vessels. Image capture, CNV area measurement, and exclusions (see below) were performed with randomized samples or data by scientists masked to the treatment group.

Compound Administration

Test articles injected intravitreally (IVT) were administered immediately after laser pulse application. A sclerotomy was made with a 30-gauge needle approximately 1.5 mm below the limbus. A 33-gauge blunt-tipped needle attached to a 10-μL syringe (Hamilton Co., Reno, NV, USA) was then inserted into the vitreous space through the sclerotomy, and 1.5 μL of the test article was administered under direct visualization of a surgical microscope. IVT injections of test articles were administered bilaterally.

Test articles that were administered by oral gavage, IP injection, IV injection, or as eyedrops had doses starting approximately 1 hour before lasering, unless described otherwise.

Material Information

Nineteen-mer and 21-mer small interfering RNA (siRNAs) targeting coagulation factor VII and a 21-mer siRNA targeting an influenza virus replication gene were injected into the vitreous at a concentration of 1 or 3 mg/mL, thereby administering 1.5 or 4.5 μg of siRNA to the vitreous. Chemical modifications to the siRNA and the RNA sequence used are described in Supplementary Table S1.

The C5a receptor antagonist PMX53 (also known as "AcF(OPdChaWR") was synthesized as described previously.[8] For IVT, IV, and IP studies, PMX53 was formulated with either 5% or 10% ethanol in sterile water. For IV and IP dosing studies, PMX53 or vehicle (ethanol in sterile water) was injected starting on day 0 and continued daily through day 6. Intravenous dosing was 10 mg/kg, and IP dosing was 10 and 30 mg/kg. For IVT dosing, PMX53 or vehicle was administered by a single injection into the vitreous after laser application. The PMX53 concentration was 3, 5, or 10 mg/mL, and IVT doses were 4.5, 7.5, or 15 μg per eye.

Cobra venom factor (CVF; Quidel, San Diego, CA, USA) was reconstituted in sterile PBS, and mice were injected IP with 4 units of CVF or PBS starting 2 days before laser pulse application. Injections continued daily until day 6 (9 injections in total).

The low-molecular-weight (LMW) VEGF receptor inhibitor pazopanib was synthesized as previously described.[9] Pazopanib or vehicle (0.5% methylcellulose, 0.1% Tween 80 in sterile water) was administered daily by oral gavage at doses ranging from 3 to 300 mg/kg in 3 independent experiments.

Three orally bioavailable LMW VEGF receptor inhibitors (PTK787, BAW2881, and BFH772)[10–12] were independently used in multiple studies as positive controls. PTK787 was dissolved in polyethylene glycol (PEG) 300 diluted with saline, 1:1, before dosing. The proprietary compound BFH772 was formulated in 10% ethanol and 90% PEG400, and the proprietary inhibitor BAW2881 was formulated in 20% of 10% ETPGS (D-alpha tocopheryl PEG 1000 succinate) and 80% of PEG400 for dosing by oral gavage.

The proprietary LMW VEGF receptor inhibitor UF-61-QB443 was formulated in sterile 1% carboxymethylcellulose (CMC) at 10 mg/mL for IVT injection. Recombinant human $VEGF_{165}$ (Peprotech, Rocky Hill, NJ, USA) was reconstituted in sterile saline to a concentration of 0.5 mg/mL for IVT injection. Triamcinolone acetonide (PCCA, Houston, TX, USA) was formulated in sterile 0.5% hydroxypropylmethyl cellulose at 5 mg/mL for IVT injection. Dexamethasone (Sigma-Aldrich, St. Louis, MO, USA) was formulated in sterile 0.5% CMC at 10 mg/mL for IVT injection. The proprietary anti-mouse VEGF antibody 4G3 was formulated in sterile PBS for IP injection.

C5-deficient mice ($C5^{-/-}$; B10.D2-Hc0 H2d H2-T18c/oSnJ; stock number 000461) and sex and age-matched wild-type C5-

sufficient controls (B10.D2-Hc1 H2d H2-T18c/nSnJ; stock number 000463) were purchased from JAX.

C3 KO mice (B6.129S4-C3^{tm1Crr}/J stock number 003641) and two types of age-matched and sex-matched control mice, C57BL/6J (stock number 000664) and B6129SF2/J (stock number 101045), were purchased from JAX.

C3 KO mice (B6.129 background; JAX) were subsequently bred and maintained at Taconic. The C3 KO mice (B6.129S4-C3^{tm1Crr}/J) were crossed to C57BL/6JBomTac animals (wild-type for Crb1^{rd8}) to generate heterozygotes. Heterozygote matings were performed to generate both C3 KO and wild-type founders. The genotype of homozygote KO and wild-type breeder mice were confirmed at Taconic by PCR analysis. Absence of the mutation in the Crb1^{rd8} gene was also confirmed by PCR analysis. Age- and sex-matched C3 KO and wild-type mice that were generation 5 (G5) from the interbred founders were studied in the laser-induced CNV assay.

Absence of C3 or C5 in KO mice was confirmed by Western blot analysis of mouse plasma with a C3 or C5 antibody in a subset of mice. The C5 antibody was mouse complement component C5a affinity-purified polyclonal antibody, goat immunoglobulin G (IgG; code AF2150; R&D Systems, Inc., Minneapolis, MN, USA), and the C3 antibody was mouse complement C3d biotinylated affinity-purified polyclonal antibody, goat IgG (code BAF2655; R&D Systems).

Application of Exclusion Criteria

Each eye typically generated 3 data points corresponding to the areas of 3 individual CNV lesions. In a typical study, a cohort of 10 mice per group would optimally provide 60 data points. However, a lesion was excluded if (1) there was choroidal hemorrhage encroaching on the lesion; (2) the lesion was linear instead of circular, a consequence of a deflected ("split") laser impact; (3) the lesion had fused with another lesion; (4) the lesion had a size indicating it was an outlier lesion as defined below; or (5) the lesion was the only lesion in an eye (i.e., if 2 of the 3 lesions in an eye were excluded, then all lesions in that eye were excluded). Representative images of excluded CNV lesions are shown in Supplementary Figure S1.

An outlier lesion fell was categorized as (1) "too big," that is, it was more than 10,000 μm^2 in area and was more than 5 times larger than the next biggest lesion in the eye (for reference, the mean area of CNV in a control group typically ranged from 10,000 to 20,000 μm^2); (2) "too small," that is, it was less than 1/5 the area of the next smallest lesion in the eye; this criterion applied only if at least 1 lesion in the eye was more than 5000 μm^2; or (3) "too different," that is, after all of the lesions in a specific treatment group were measured, the lesion's area was 5-fold greater than the mean for that group; this criterion applied only for lesions that were $\geq$5000 μm^2. Representative examples of application of size criteria are shown in Supplementary Table S2.

Other reasons for excluding lesions were (1) death of a mouse before the end of an experiment; (2) failure of the IV injection of the vascular label; (3) media opacities precluding accurate laser application (e.g., a pre-existing corneal scar or cataract); in this case the fellow eye could still be included; (4) damage to the CNV lesion during tissue processing (i.e., poor quality of the tissue during processing so that the lesion could not be fully delineated); or (5) inability to locate a CNV lesion during the imaging of an eyecup.

To illustrate the impact of excluded data, Supplementary Table S3 summarizes the data points excluded and the reasons for the exclusions from placebo-treated mice from 10 recent experiments.

Statistics

One-way ANOVA was performed using Prism version 6 software (GraphPad, Inc., San Diego, CA, USA) for Windows (Microsoft, Redmond, WA, USA) with Dunnet's post hoc analysis test.

The mean CNV area in the placebo group, as well as the pooled standard deviation (SD), was calculated for 10 experiments in Prism software. Power calculations based on the mean CNV area $\pm$ pooled SD were performed using SYSTAT version 13 (SYSTAT, Inc., Chicago, IL, USA) for an unpaired *t* test with a significance level of 0.05 and an 80% power and a 90% power to detect a 50% difference in mean, assuming that the SDs were the same in placebo and treated groups.

The ED_{50} curve was generated in Excel/XLfit (version 5.2.0.0:ID Business Solutions Ltd., Guildford, UK) with results from three individual dose response efficacy experiments, using a dose-response one-site fit, with sigmoidal dose-response model [fit = (A+((B–A)/(1+((C/x)^D)))))], without parameter constraints (extrapolation allowed).

Results

Dose Selection of a VEGF Receptor Inhibitor

Proprietary LMW VEGF receptor inhibitors (PTK787, BAW2881, BFH772 and UF-61-QB443) that inhibit VEGF receptor-2 or a proprietary antibody that neutralizes VEGF (4G3) were used as positive controls.[11,12] In a fluorescence resonance energy transfer human enzymatic assay, compounds BFH772 and BAW2881 inhibited VEGF receptor-2 enzymatic activity with a 50% inhibitory concentration (IC_{50}) of 4 nM and compound UF-61-QB443 with an IC_{50} of 8 nM (LanthaScreen kinase activity assay; LifeTechnologies, Grand Island, NY, USA). In a scintillation proximity assay of human enzymatic activity, PTK787 inhibited VEGF receptor-2 kinase activity with an IC_{50} of 37 nM.[10] Compound 4G3 is a human Fab converted to a full-length IgG antibody with a mouse IgG1 Fc tail. The 4G3 binds to mouse $VEGF_{164}$ with a K_d of 10 pM, as measured by Biacore (GE Healthcare Bio-Sciences Pittsburgh, PA, USA; data not shown) and neutralizes mouse VEGF binding to human VEGFR-2 with an EC_{50} of 0.15 nM in a binding assay (ELISA; MSD, Rockville, MD, USA). To validate our in vivo methodology, we assessed the dose-response of pazopanib, a LMW VEGF receptor inhibitor,[9,13,14] in three independent experiments. Compared to vehicle-treated mice that served as negative controls, the ED_{50} of orally administered pazopanib was 63 mg/kg (Fig. 1, and see Supplementary Figs. S2–S4). Similar dose-response studies were performed for the proprietary LMW VEGF receptor inhibitors that we used as positive controls. LMW VEGF receptor inhibitors BFH772, BAW2881, and PTK787 have ED_{50} values of $\sim$2, 4, and 60 mg/kg, respectively, when administered orally once a day.

Statistical Power

Based on the mean CNV area from 10 experiments and the pooled SD, for an unpaired two-tailed *t*-test, 41 data points have approximately 80% power and 55 points 90% power with an alpha of 0.05 to observe a 50% difference in means (Supplementary Table S4).

Effect of siRNA

IVT injection of a 21-nucleotide siRNA but not a 19-nucleotide siRNA is reported to inhibit CNV through non-specific activation of Toll-like receptor-3.[5] We evaluated the effects of

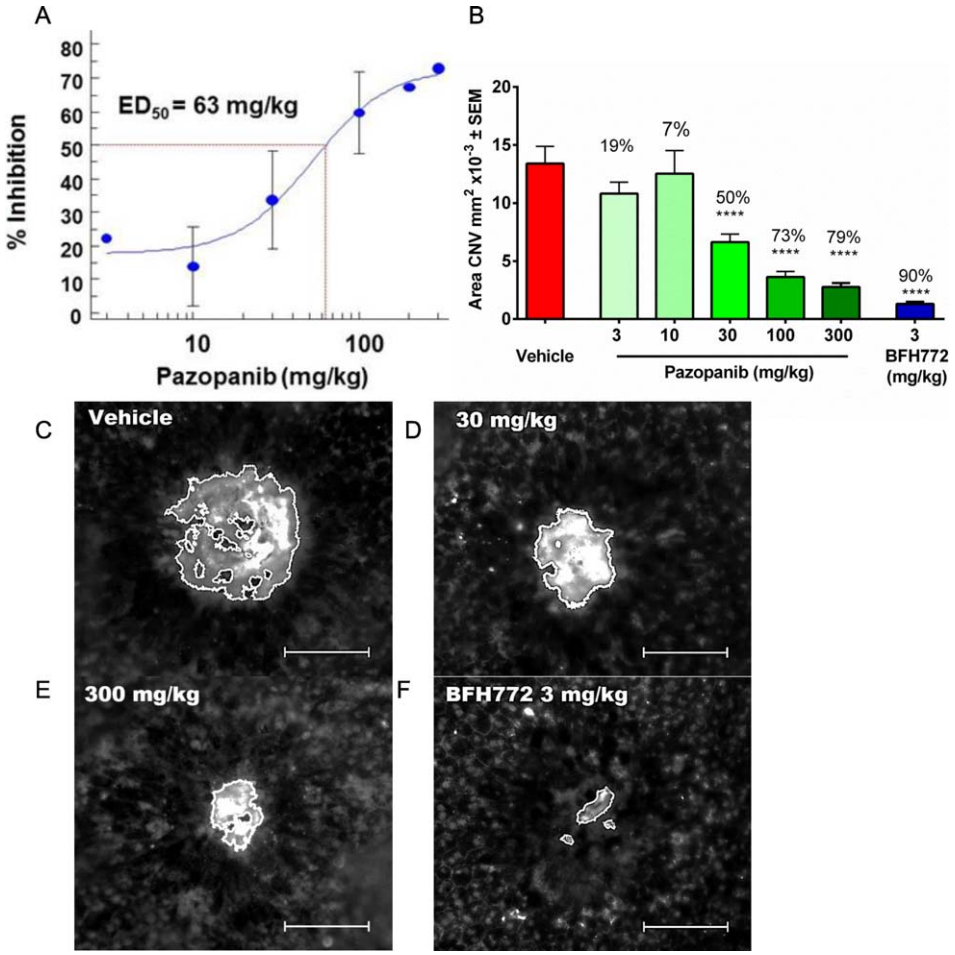

Figure 1. (**A**) The dose-response relationship between daily orally dosed pazopanib and the reduction in CNV area is shown. Data points are mean percent inhibition averaged across 3 independent experiments, each of which tested 4 to 6 doses. The ED_{50} of pazopanib is 63 mg/kg. Error bars indicate ±1 SD. Doses assessed in fewer than 3 studies do not have error bars; experimental details for the 3 studies are given in Supplementary Figures S2 through S4. (**B**) The mean ± SEM area of CNV from one representative experiment evaluating the inhibition of laser-induced CNV of mice orally dosed with vehicle, pazopanib, or a positive control, BFH772 (a LMW VEGF receptor inhibitor). The number *above* each bar is the percentage of inhibition relative to the average CNV area in vehicle-treated mice. For doses ≥30 mg/kg, differences in CNV area are significantly different from those of vehicle-treated mice (****$P < 0.0001$ by ANOVA with Dunnett's post hoc analysis). (**C–F**) Representative fluorescent images are shown of CNV 7 days after laser treatment of mice dosed daily with vehicle, pazopanib, or BFH772. (**C**) Vehicle; (**D**) 30 mg/kg pazopanib; (**E**) 300 mg/kg pazopanib; (**F**) 3 mg/kg BFH772. Lesions are *outlined* by analysis software (see Methods). *Scale bars*: 100 μm.

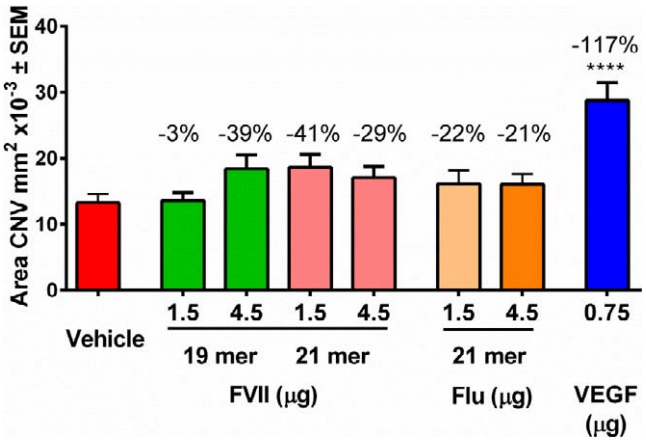

Figure 2. Intravitreal administration of 19-mer and 21-mer siRNAs did not significantly increase CNV area. *Bars* indicate mean ± SEM CNV areas from one experiment comparing mice injected IVT with saline (Veh) or siRNAs. Mice were injected IVT with 1.5 μL of saline, 1.5 or 4.5 μg of 19-mer or 21-mer siRNA targeting factor VII, or 1.5 or 4.5 μg of 21-mer siRNA targeting an influenza virus replication gene, or 750 ng of $VEGF_{165}$. All injections were given immediately after laser photocoagulation. The number *above* each bar is the percentage of change compared to the vehicle–treated group. CNV area was not significantly different in mice injected with siRNA compared to those injected with saline but was increased in mice injected with VEGF (****$P < 0.0001$).

one 19-nucleotide and two 21-nucleotide siRNAs administered by IVT injection on laser-induced CNV. The siRNAs had sequences derived from the genes of coagulation factor VII and an influenza virus. The doses and dose frequencies were similar to those described by another group[5] with one experiment testing doses one-half log (i.e., 3×) higher than what was previously published.

The 19- and 21-nucleotide siRNAs had no statistically significant effect on the area of CNV compared to control mice that were injected with vehicle ($P > 0.05$) (Fig. 2, and see Supplementary Figs. S5, S6). RPE atrophy was not observed in the mice injected with siRNA. IVT injection of 750 ng of

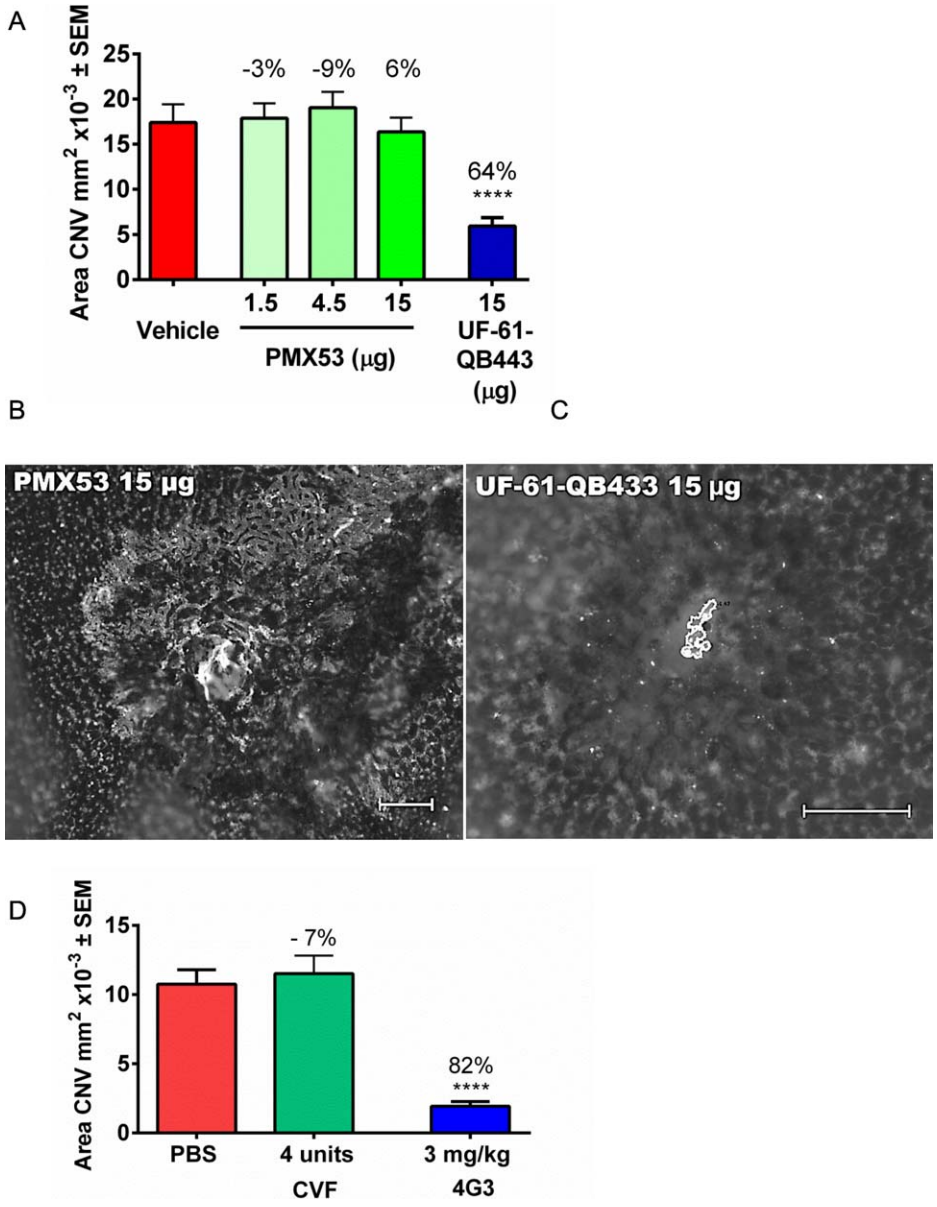

Figure 3. (**A**) IVT administration of PMX53, a peptide antagonist of the C5a receptor, did not inhibit laser-induced CNV at any dose. The *number above* each bar is the percentage of inhibition compared to that of the vehicle-treated group. Mice received an injection of vehicle, PMX53, or a positive control, UF-61-QB433 (a LMW VEGF receptor inhibitor). CNV area was inhibited by the positive control compound ($P < 0.0001$). Similar results were obtained in two other experiments. (**B**) Representative image of RPE atrophy in an eye injected IVT with PMX53 (*scale bars*: 100 μm). Lesions in these atrophic areas were excluded from analysis. (**C**) Representative image of an inhibited CNV from an eye dosed with 15 μg IVT of UF-61-QB433; the RPE is healthy. (**D**) Systemic administration of cobra venom factor (CVF) did not inhibit laser-induced CNV. Mice received i.p. injections of PBS, CVF, or a positive control drug (anti-VEGF antibody 4G3). CNV area was inhibited in the positive control group ($P < 0.0001$). Similar results were obtained in a repeated experiment ($^{****}P < 0.0001$).

$VEGF_{165}$ after laser approximately doubled the area of CNV ($P < 0.0001$).

Effect of Pharmacologic Inhibition of Complement Factors

Complement factor C5a is a proinflammatory protein that recruits leukocytes by activating the C5a receptor (C5aR), a 7-transmembrane G protein-coupled receptor. IVT injection of PMX53, a cyclic peptide inhibitor of C5aR, was reported to inhibit laser-induced CNV in mice.[6] PMX53 is reported to inhibit in vitro C5a activity in human inflammatory cells and also to protect rodents from inflammatory diseases.[15]

In separate experiments, we evaluated PMX53 by IVT, IV, and IP administration. IVT administration of this C5a receptor antagonist had no effect on neovascularization. Non-uniform atrophy of the RPE was dose dependently observed in many eyes receiving the drug (Fig. 3, and see Supplementary Figs. S7–S9). When RPE atrophy was present in the area of the laser pulse impact, the CNV lesions were not fully discernible and therefore were excluded. Approximately 50% of CNV lesions in mice injected with 15 μg PMX53 were either excluded or lesions were not measurable. For mice injected with IVT vehicle in the same experiments, approximately 15% of CNV lesions were not measured or were excluded. If the reduced fluorescence in these affected areas had been interpreted as

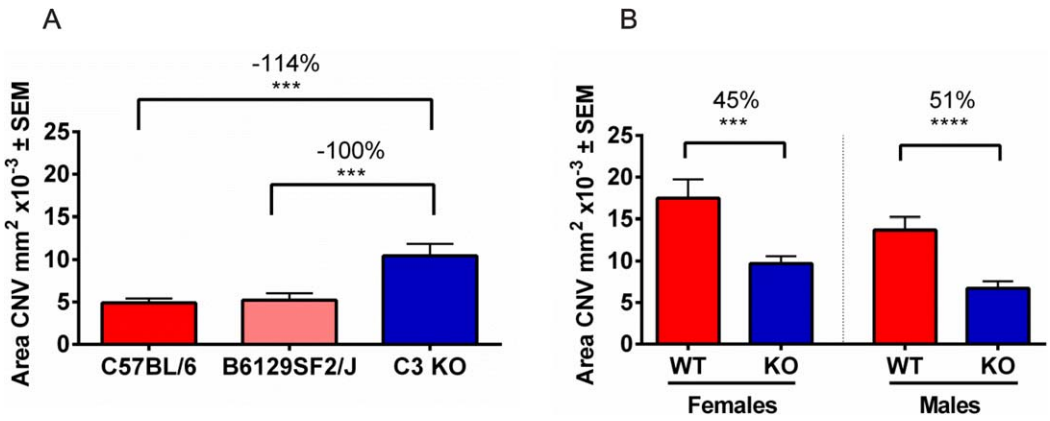

FIGURE 4. Origin of the mice and types of wild-type (WT) controls influence interpretation of the effect of lack of complement factor C3 effect on laser-induced CNV. (**A**) JAX C3 KO mice had larger average CNV area than 2 strains (C57BL/6J and B6129SF2/J) of age- and sex-matched control mice from the JAX. Similar results were observed in a repeated experiment. (**B**) Taconic C3 KO mice have significantly reduced CNV areas compared to age- and sex-matched control mice from Taconic. Similar results were observed in a repeated experiment. *Bar graphs* are mean ± SEM areas of CNV. For both figures, the number *above the line* is the percentage of change compared to that of the respective control group (***$P < 0.001$, ****$P < 0.0001$).

inhibition of CNV, one might have concluded that the compound was efficacious. Atrophy was not observed in eyes dosed with vehicle. In addition, neovascularization in mice dosed IP or IV with PMX53 did not differ from that in IP or IV vehicle dosed control mice (Supplementary Figs. S10–S13).

CVF is a nontoxic, complement-activating component of cobra venom that forms a stable C3 convertase with factors D and B. IP administration of CVF will systemically deplete C3, functionally inhibiting complement activity. Systemic CVF administration has been reported to fully suppress laser-induced CNV.[4] In our experience, a single IP injection of CVF depletes mouse plasma C3 for ≥48 hours (data not shown). In contrast to the published findings, CVF did not reduce CNV area ($n = 2$ experiments, $P > 0.05$) (Fig. 3, and see Supplementary Figs. 14, 15).

Effect of Genetic Knock-Out of Complement Factors

Published studies report a dramatic reduction in the incidence of laser-induced CNV in $C3^{-/-}$ or $C5^{-/-}$ mice compared to control mice.[4,7] JAX C3 knockout (KO) mouse is from a mixed C57BL/6 and SV129 background. JAX currently recommends a C57BL/6J mouse as an "approximate control" (http://jaxmice.jax.org/strain/003641.html). Published experiments involving $C3^{-/-}$ mice[4] used "(129 x C57BL/6)F1" mice as a control. We therefore decided to compare C3 KO mice with two wild-type control strains. We found a 95% increase in CNV area in C3 KO mice compared with C57BL/6J wild-type controls (two experiments, $P \leq 0.01$). We found a 65% increase in CNV area in the C3 KO mice compared to B6129SF2/J wild-type controls (one experiment, $P > 0.05$, one experiment $P < 0.001$) (Fig. 4, and see Supplementary Figs. S16, S17). B6129SF2/J mice are the offspring of a C57BL/6J and 129S1/SvImJ cross (http://jaxmice.jax.org/strain/101045.html).

We subsequently compared a line of C3 KO and wild-type control mice, both crossbred from JAX C3 KO and Taconic C57BL/6 mice. In contrast to the findings in JAX C3 KO mice, the average CNV area was smaller in crossbred C3 KO mice than in the crossbred wild-type controls. Male C3 KO mice had an average reduction of 50.5% in CNV area ($n = 2$ experiments, $P \leq 0.003$) compared to wild-type males. Female mice had an average reduction of 34.6% compared to female wild-type controls ($n = 2$ experiments, $P = 0.054$ and 0.001) (Fig. 4, and see Supplementary Figs. S18, S19).

$C5^{-/-}$ mice had a small (approximately 30%) increase in CNV area compared to C5 sufficient controls that was statistically significant ($P = \leq 0.04$) (Fig. 5, and see Supplementary Figs. S20, S21). This is in contrast to the substantial decrease in CNV reported by others who evaluated the same $C5^{-/-}$ strain.[7]

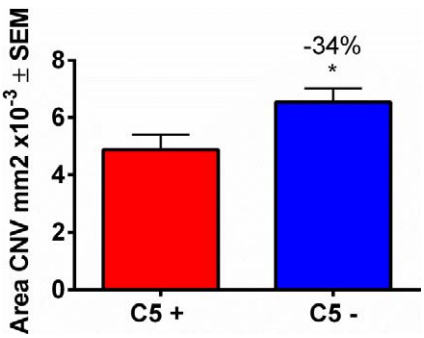

FIGURE 5. CNV areas are increased in $C5^{-/-}$ mice compared to those in C5-sufficient (C5+) mice. *Bar graphs* are mean ± SEM CNV area (unpaired *t*-test, $P = 0.02$). A similar result was observed in a repeated experiment. The number *above the bar* is the percentage of inhibition relative to that of the average area of neovascularization in the C5+ mice (*$P < 0.05$).

Variation of Neovascularization Depending on the Origin of Mice

During the courses of experiments described here and by others, we obtained wild-type C576BL/6 mice from three vendors: Taconic, JAX, and Charles River Laboratory. The mice were between 7 and 14 weeks old, and most were between the ages of 8 and 10 weeks. We retrospectively reviewed data from placebo-treated or untreated wild-type female mice from the 3 vendors in 132 experiments from 2007 to 2010. The areas of neovascularization in mice from Charles River Laboratories and JAX were significantly less than those in mice from Taconic (Fig. 6).

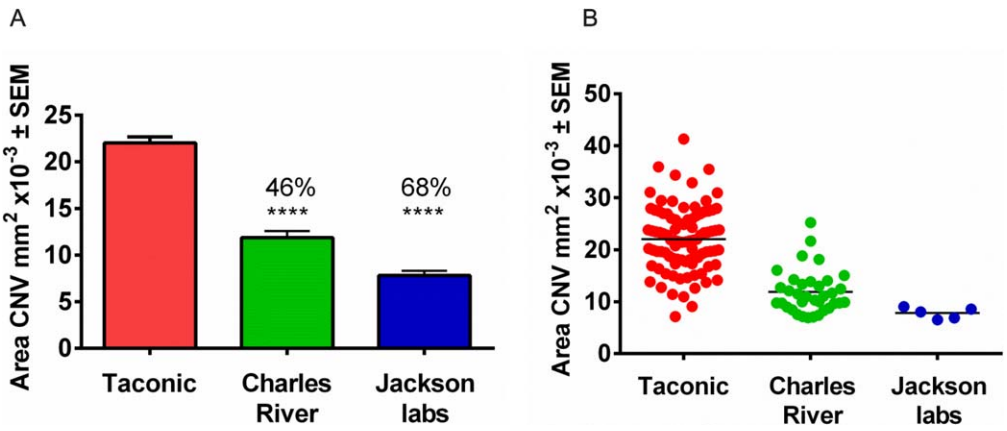

FIGURE 6. Mice from different vendors produce laser-induced CNV areas of different magnitudes. (**A**) *Bar graph* and (**B**) *dot plot* of CNV areas in placebo-treated and naïve (untreated) mice from Taconic (92 experiments, $n = 920$ mice), Charles River (35 experiments, $n = 350$ mice), and JAX (5 experiments, $n = 50$ mice). Mice were dosed with placebos by oral, topical, or intraperitoneal routes of administration (see Supplementary Fig. S22; CNV areas in Taconic female mice dosed by different routes of administration were similar to those in treated naïve mice). Experiments were conducted between 2007 and 2010. Average CNV areas were significantly smaller in mice from Charles River and JAX than in mice from Taconic (****$P < 0.0001$).

Reproducibility of CNV Area With Different Laser Operators

We retrospectively reviewed the results of 92 experiments with female wild-type control mice obtained from one vendor (Taconic). These experiments were conducted over the course of 4 years (2007–2010). During these studies, four members of our group administered laser burns according to the same protocol and the same laser settings. There was no predetermined pattern as to which scientist was assigned to operate the laser in each experiment. For this retrospective review, we compiled results from the negative control mice that received placebos either by IP, oral, or topical administration or that received no treatment. The route of administration of placebo did not significantly alter the CNV area (Supplementary Fig. S22). There were no statistically significant differences among areas of neovascularization generated by each of the four scientists compared to the others (Fig. 7).

Changes Over Time in the Responses of Mice

Upon reviewing CNV areas in Taconic mice over time, we noticed an abrupt and persistent change in CNV responses beginning in the last study conducted in 2010 (this cohort of mice were born in late September 2010). We therefore performed an additional retrospective analysis of average CNV areas in placebo-treated or untreated C57BL/6 Taconic female mice in 114 experiments performed between 2007 and 2012. Laser operators in 2011 and 2012 overlapped with operators in 2010. Average CNV areas in negative control mice between 2007 and 2010 were similar (19.1–23.6 $mm^2 \times 10^{-3}$). Average CNV areas in negative control mice in 2011 and 2012 (12.6 and 12.2 $mm^2 \times 10^{-3}$) were almost 50% reduced compared to the average CNV area in 2010 (Supplementary Fig. S23). The average percentage of inhibitions in mice treated with positive control drugs compared to placebos were similar for these years (data not shown).

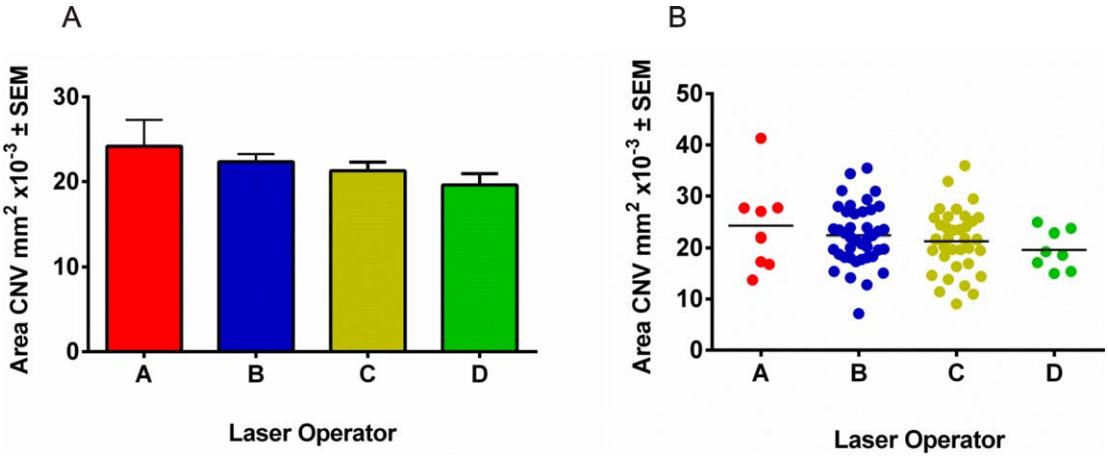

FIGURE 7. Laser CNV is not influenced by the laser operator. Laser photocoagulation was applied by scientists designated A, B, C, and D. Average CNV areas are similar for the four scientists ($P > 0.05$, one-way ANOVA with a Dunnett post hoc analysis). Experiments were conducted between 2007 and 2010. There were 8 to 41 experimental runs per scientist. (**A**) *Bar graph* of mean ± SEM CNV area per laser operator and (**B**) *dot plot* of the mean CNV area in placebo-treated or naïve (untreated) groups of mice are shown.

Table. Guidelines for Minimizing Bias and Reducing Type 1 Errors for Experiments

Validate the assay with a positive control that shows a clear dose-response relationship
Perform power calculations to ensure experiments are adequately powered
Define predetermined exclusion and inclusion criteria for data points; exclude data while masked to the group
Perform analyses of masked data
Repeat experiments at least once
Assess the dose–response relationship of therapeutic reagents
Include a positive control in each run of the experiment
Use litter mate controls from breeding of congenic heterozygote parents for gene KO experiments

Discussion

Although considered "routine," the laser-induced CNV model requires careful design and implementation.[16,17] In developing our methodology, we used many experiments to optimize the laser application, vascular label, dissection and fixation techniques, exclusion criteria, masking methodology, and measurement of CNV area. Our experience is that the lowest power and shortest duration of laser that consistently ruptures Bruch's membrane yields the optimal CNV lesions. When the spot power or spot burn duration is increased, CNV lesions are associated with increased tissue debris and poorer tissue quality, making measurements less precise. Increased spot power or duration of pulse does not increase CNV area. Our exclusion criteria were developed based on validation studies to remove data that potentially confounded the real effect of a study condition. For example, occasionally a laser burn will yield a CNV lesion many times larger than the fellow CNV lesions in the eye. This may be related to a hemorrhage or proximity of the laser pulse to a large choroidal vessel. Occasionally, a CNV lesion may be displaced during dissection, mimicking the appearance of total inhibition of one lesion. These outliers can skew data, suggesting a drug effect, when in fact none may exist. Removing these outliers improved the reliability of our data. In a typical group of 10 mice, approximately 80% of the 60 possible lesions could be analyzed and assessable (Supplementary Table S3). IV vascular labeling identifies physiologically perfused vessels and, with practice, is a quick and reliable procedure. Image capture of CNV lesions is fast, taking approximately 1 to 2 minutes per eye. Semiautomated CNV area measurement is straightforward and takes less than an 1 hour for a 100-mouse study. Confocal imaging to measure CNV volume, in contrast, is slower. To increase objectivity, all data capture and analysis are performed with randomized data by a scientist masked to the treatment groups. We have been able to reproducibly generate dose-response curves for LMW VEGF receptor inhibitors and generate consistent CNV areas in placebo-treated mice with different laser operators. This reproducibility of our data gives confidence that our methods are appropriate for studying laser-induced CNV.

We have estimated the power of our sample sizes based on the SD of lesion areas in placebo-treated mice. The Table summarizes the procedures we use to optimize the model. Pazopanib at a daily oral dose of 100 mg/kg consistently reduced the area of neovascularization by $\geq$50%. This is a suitable molecule and dose for use as a positive control for researchers who do not have access to proprietary VEGF receptor inhibitors.

In the hundreds of experiments that we have conducted in the last 7 years, we have occasionally encountered reagents that provide significant deviations from the control group (e.g., ~50% inhibition) but no significant deviation in a second or third experiment. The frequency of such non-reproducible results is roughly in accord with the type 1 (false positive) error that we expect from our power calculations used to determine the number of animals per arm.

Some of our results substantially and reproducibly differ from results reported by other groups. It is possible that some of the differences between our results and published findings could be related to differences in methodology. Different lasers or laser parameters, as used by other laboratories, may induce different ocular responses to a laser pulse. Isolectin labeling of blood vessels post mortem would label non-perfused blood vessels and microglia, thereby leading to the measurement of larger lesion areas. Confocal microscopy measures CNV volume instead of area. The discrepancies could alternatively be due to type 1 error in those laboratories. In order to be confident of decisions based on the laser-induced CNV model, we do not consider results from our group or from other groups valid unless we obtain comparable results in at least two separate, similarly conducted experiments that were conducted according to the standards recommended by Landis et al.[18] and ideally conform to the guidelines in the Table.

CNV areas can vary between control cohorts of mice, and therefore, the controls used in experiments involving transgenic mice or specific strains of mice are important. Mouse genetic background may influence the ocular response to laser and other pharmacodynamic responses.[19,20] We have observed that even wild-type mice from a single vendor can respond to laser photocoagulation with different CNV areas over time, possibly due to genetic drift or changes in diet or environment that the mice experience at the vendor. We do not think the change in the responses in Taconic mice was due to calibration anomalies of our laser as we did not observe a change in CNV areas in the rat studies that were being conducted concurrently. Optimally, both wild-type controls and genetically modified mice for an experiment come from the same matings of heterozygote parents. The importance of controls is highlighted in our observations with C3 KO mice. In one set of experiments, we observed convincing exacerbation of CNV in C3 KO mice compared to non-littermate wild-type controls. In contrast, in experiments with mice produced by breeding heterozygotes, we observed partial but convincing CNV inhibition. Both observations could be due to differences in background genotype, rather than the lack of complement factor C3. In contrast to published findings, we conclude that laser-induced CNV forms in the absence of C3, but we cannot determine if C3 modulates CNV area. We are currently backcrossing C3 KO mice to Taconic wild-type mice (all mice are $Crb1^{rd8}$ wild-type). When congenic C3 KO and C57BL/6 mice are available, we plan to assess CNV in C3 KO and wild-type litter mate controls.

Although the main point of this report was to highlight how to optimize the mouse laser-induced CNV model, commentary on the relevance of our results for AMD is in order. Laser-induced CNV is a VEGF-dependent process, as indicated by how dramatically it is inhibited by potent drugs that block VEGF or its receptor, and how it is exacerbated by ocular application of VEGF. The average maximal inhibition of CNV we have observed with an anti-VEGF antibody is approximately 70% to 80%, and we observe 80% to 95% inhibition with LMW VEGF receptor inhibitors. The larger effect observed with VEGF receptor inhibitors may be related to their activity against other receptor tyrosine kinases including all three VEGF receptors and kinases that have functions related to inflammation or pericyte recruitment.[21] Enhanced ocular exposure of a small molecule inhibitor relative to an antibody at the choriocapillaris and retinal pigment epithelium may also

explain the improved efficacy. A small-molecule tyrosine kinase inhibitor may therefore have greater ability to treat neovascular AMD than large-molecule therapies that block the ligand VEGF or other ligands in the VEGF family.

There is compelling evidence that the complement pathway has a role in AMD, based primarily on associations between the risk for the disease and genotypes at loci encoding complement factors H, B, I, C2, C3, C5, and C9.[22–26] Alleles associated with AMD encode variants of the complement factors that appear to mediate greater activity of the pathway compared to the comparator alleles.[27] It remains unclear whether high activity of the complement pathway only increases the risk of developing AMD or whether it also increases the chance that the disease will progress from its intermediate forms to its advanced forms such as CNV or geographic atrophy. Superimposed environmental factors such as tobacco smoke and variations in other biochemical pathways are likely important as well.[22,28] Experiments in which the complement pathway is manipulated in the mouse laser-induced CNV model do not incorporate the numerous non-complement factors that have a role in AMD. Thus, exacerbation of CNV in some experiments of mice completely lacking a complement factor does not necessarily indicate that complement inhibition would adversely affect patients with neovascular AMD. An equally reasonable and perhaps more likely explanation is that the CNV induced by laser injury is pathophysiologically distinct from the CNV which forms in aged human eyes with AMD and a chronically, modestly altered complement pathway. In short, results from modulation of complement activity in the mouse laser-induced CNV model might inaccurately predict the effect of complement inhibitors in eyes with neovascular AMD.

Acknowledgments

The authors thank Yiqin Wang and Bijan Etemad-Gilbertson for characterizing the 4G3 antibody with Biacore and ELISA assays.

Disclosure: **S.H. Poor**, Novartis Institutes for Biomedical Research (E); **Y. Qiu**, Novartis Institutes for Biomedical Research (E); **E.S. Fassbender**, Novartis Institutes for Biomedical Research (E); **S. Shen**, Novartis Institutes for Biomedical Research (E); **A. Woolfenden**, Novartis Institutes for Biomedical Research (E); **A. Delpero**, Novartis Institutes for Biomedical Research (E); **Y. Kim**, Novartis Institutes for Biomedical Research (E); **N. Buchanan**, Novartis Institutes for Biomedical Research (E); **T.C. Gebuhr**, Novartis Institutes for Biomedical Research (E); **S.M. Hanks**, Novartis Institutes for Biomedical Research (E); **E.L. Meredith**, Novartis Institutes for Biomedical Research (E); **B.D. Jaffee**, Novartis Institutes for Biomedical Research (E); **T.P. Dryja**, Novartis Institutes for Biomedical Research (E)

References

1. Ishibashi T, Miller H, Orr G, Sorgente N, Ryan SJ. Morphologic observations on experimental subretinal neovascularization in the monkey. *Invest Ophthalmol Vis Sci*. 1987;28:1116–1130.
2. Nehemy MB, Torqueti-Costa L, Magalhaes EP, Vasconcelos-Santos DV, Vasconcelos AJ. Choroidal neovascularization after accidental macular damage by laser. *Clin Experiment Ophthalmol*. 2005;33:298–300.
3. Krzystolik MG, Afshari MA, Adamis AP, et al. Prevention of experimental choroidal neovascularization with intravitreal anti-vascular endothelial growth factor antibody fragment. *Arch Ophthalmol*. 2002;120:338–346.
4. Bora PS, Sohn J-H, Cruz JMC, et al. Role of complement and complement membrane attack complex in laser-induced choroidal neovascularization. *J Immunol*. 2005;174:491–497.
5. Kleinman ME, Yamada K, Takeda A, et al. Sequence- and target-independent angiogenesis suppression by siRNA via TLR3. *Nature*. 2008;452:591–597.
6. Nozaki M, Raisler BJ, Sakurai E, et al. Drusen complement components C3a and C5a promote choroidal neovascularization. *Proc Natl Acad Sci U S A* 2006;103:2328–2333.
7. Bora NS, Kaliappan S, Jha P, et al. Complement activation via alternative pathway is critical in the development of laser-induced choroidal neovascularization: role of factor B and factor H. *J Immunol*. 2006;177:1872–1878.
8. March DR, Proctor LM, Stoermer MJ, et al. Potent cyclic antagonists of the complement C5a receptor on human polymorphonuclear leukocytes. Relationships between structures and activity. *Mol Pharmacol*. 2004;65:868–879.
9. Harris PA, Boloor A, Cheung M, et al. Discovery of 5-[[4-(2,3-dimethyl-2H-indazol-6-yl)methylamino]-2-pyrimidinyl]amino]-2-methyl-benzenesulfonamide (Pazopanib), a novel and potent vascular endothelial growth factor receptor inhibitor. *J Med Chem*. 2008;51:4632–4640.
10. Wood JM, Bold G, Buchdunger E, et al. PTK787/ZK 222584, a novel and potent inhibitor of vascular endothelial growth factor receptor tyrosine kinases, impairs vascular endothelial growth factor-induced responses and tumor growth after oral administration. *Cancer Res*. 2000;60:2178–2189.
11. Halin C, Fahrngruber H, Meingassner JG, et al. Inhibition of chronic and acute skin inflammation by treatment with a vascular endothelial growth factor receptor tyrosine kinase inhibitor. *Am J Pathol*. 2008;173:265–277.
12. Meingassner JG, Fahrngruber H, Kowalsky E, et al. NVP-BFH772, a potent inhibitor of VEGF receptor tyrosine kinases, is effective in models of skin inflammation. In: Annual Meeting of the Society for Investigative Dermatology; May 4 to 7, 2011. Phoenix, AZ. Abstract 480.
13. Amparo F, Sadrai Z, Jin Y, et al. Safety and efficacy of the multitargeted receptor kinase inhibitor pazopanib in the treatment of corneal neovascularization. *Invest Ophthalmol Vis Sci*. 2013;54:537–544.
14. McLaughlin MM, Paglione MG, Slakter J, et al. Initial exploration of oral pazopanib in healthy participants and patients with age-related macular degeneration. *JAMA Ophthalmol*. 2013;131:1595–1601.
15. Subramanian H, Kashem SW, Collington SJ, Qu H, Lambris JD, Ali H. PMX-53 as a dual CD88 antagonist and an agonist for mas-related gene 2 (MrgX2) in human mast cells. *Mol Pharmacol*. 2011;79:1005–1013.
16. Zhu Y, Lu Q, Shen J, et al. Improvement and optimization of standards for a preclinical animal test model of laser induced choroidal neovascularization. *PLos ONE* 2014;9:e94743.
17. Lambert V, Lecomte J, Hansen S, et al. Laser-induced choroidal neovascularization model to study age-related macular degeneration in mice. *Nat Protoc*. 2013;8:2197–2211.
18. Landis SC, Amara SG, Asadullah K, et al. A call for transparent reporting to optimize the predictive value of preclinical research. *Nature*. 2012;490:187–191.
19. Freeman HC, Hugill A, Dear NT, Ashcroft FM, Cox RD. Deletion of nicotinamide nucleotide transhydrogenase. A new quantitative trait locus accounting for glucose intolerance in C57BL/6J mice. *Diabetes*. 2006;55:2153–2156.
20. Mattapallil MJ, Wawrousek EF, Chan C-C, et al. The rd8 mutation of the crb1 gene is present in vendor lines of C57BL/6N mice and embryonic stem cells, and confounds ocular induced mutant phenotypes. *Invest Ophthalmol Vis Sci*. 2012;53:2921–2927.
21. Takahashi K, Saishin Y, Saishin Y, King AG, Rl, Levin, Campochiaro PA. Suppression and regression of choroidal neovascularization by the multitargeted kinase inhibitor pazopanib. *Arch Ophthalmol*. 2009;127:494–499.

22. Consortium, AMD Gene, Fritsche LG, Chen W, et al. Seven new loci associated with age-related macular degeneration. *Nature Genet*. 2013;45:433–439.
23. Baas DC, Ho L, Ennis S, et al. The complement component 5 gene and age-related macular degeneration. *Ophthalmology*. 2010;117:500–511.
24. Seddon JM, Yu Y, Miller EC, et al. Rare variants in CFI, C3 and C9 and associated with high risk of advanced age-related macular degeneration. *Nat Genet*. 2013;45:1366–1370.
25. Nishiguchi KM, Yasuma TR, Tomida D, et al. C9-R95X polymorphism in patients with neovascular age-related macular degeneration. *Invest Ophthalmol Vis Sci*. 2012;53:508–512.
26. Anderson DH, Radeke MJ, Gallo NB, et al. The pivotal role of the complement system in aging and age-related macular degeneration: hypothesis re-visited. *Prog Retin Eye Res*. 2010;29:95–112.
27. Khandhadia S, Cipriani V, Yates JRW, Lotery AJ. Age-related macular degeneration and the complement system. *Immunobiology*. 2012;217:127–146.
28. Chakravarthy U, Augood C, Bentham GC, et al. Cigarette smoking and age-related macular degeneration in the EUREYE study. *Ophthalmology*. 2007;114:1157–1163.

Investigative Ophthalmology & Visual Science